ACS OMEGA

Open Access

http://pubs.acs.org/journal/acsodf

Article

Controlling Mechanical Properties of Medical-Grade Scaffolds through Electrospinning Parameter Selection

Clayton J. Culbreath, Seth D. McCullen, and O. Thompson Mefford*

Cite This: *ACS Omega* 2024, 9, 36982−36992

Read Online

ACCESS | Metrics & More | Article Recommendations | Supporting Information

ABSTRACT: Electrospinning (ES) is a versatile process mode for creating fibrous materials with various structures that have broad applications ranging from regenerative medicine to tissue engineering and surgical mesh implants. The recent commercialization of this technology for implant use has driven the use of resorbable electrospun products. Resorbable electrospun meshes offer great promise as temporary implants that can utilize the layer upon layer method of additive manufacturing to incorporate porosity as a function of process parameters into a scaffold structure. The interconnected porosity and feature size known to ES have previously been observed to hold great potential for simulating the natural cellular environment of soft tissue. This microstructure, proper degradation kinetics, and mechanical properties combine to provide the design basis for artificial tissue structures that could aid in not only wound healing but also true tissue engineering and regenerative medicine. While current advancement in the field is understood to be limited by material properties, the importance of optimizing mechanical properties with currently available materials should not be overlooked. This work investigated the process parameter effects and interactions that control the structure−property relationship for a range of medical-grade aliphatic polyester materials with a range of intrinsic properties. An ε-caprolactone homopolymer (PCL), L-lactide homopolymer (PLLA), and Lactoflex, a copolymer with intermediate properties relative to the homopolymers, were characterized before, during, and after the additive manufacturing process. The interacting effects of process parameters, distance to collector, and dispensing rate were shown to produce variable-density, nonwoven scaffold structures. The resorbable mesh scaffolds of PLLA, PCL, and Lactoflex demonstrated a broad range of mechanical properties (approximately 1−10 MPa ultimate tensile strength and 5−390 MPa tensile modulus). Postprocessing of scaffolds demonstrated removal of solvents and preservation of micrometer-sized features. Resorbable polymers and electrospinning can produce scaffold materials with excellent features and offer tremendous potential in the field of implantable resorbable devices.

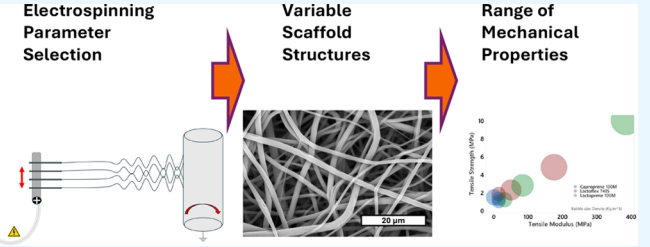

INTRODUCTION

The production and use of resorbable medical devices has increased along with the international market for medical devices that is approaching half a trillion US dollars.[1] This surge in a desire to avoid long-term risks and follow up procedures has resulted in the replacement of current implants that are not degradable, as well as the development of scaffolds previously not possible. The new possibilities, afforded by additive manufacturing techniques, have propelled the potentials in tissue engineering and regenerative medicine (TERM), allowing for targeted replacement options that offer equivalent, or improved, functional tissue for both acute and chronic needs.[2]

The distinction between healing by repair and regeneration is founded in a scaffold structure that supports and promotes the reformation of ideal cellular arrangements throughout the healing cycle. The final phase of a scaffold that promotes healthy tissue is for the scaffold to degrade and resorb, allowing the tissue structure to support itself. The term structure is inclusive and composed of, but not limited to, the polymer chain component(s), morphology (residual contaminants, crystallinity, etc.), fiber shape(s), fiber surface features, and, most pertinent to this paper, the fiber arrangement that results in an interconnected pore network (scaffold structure). Within the controls of this study, the modulated structure was quantified by the density of the samples. The need for material resorption has provided a unique opportunity for bioresorbable polymers that already have an established history in medical devices. Understanding of the currently available materials, the process optimization potentials, and the ideal tissue scaffold specifications would provide a pathway to advanced therapies that are fully successful from all perspectives.[3−5]

Aliphatic polyester materials, which make up a family of bioresorbable polymers, degrade by hydrolysis into molecules

Received: February 26, 2024
Revised: July 28, 2024
Accepted: July 30, 2024
Published: August 20, 2024

already established as metabolites. Potential aliphatic polyesters for use as scaffold materials include poly(lactide) (PLA) and poly(caprolactone) (PCL).[6−10] PLA, and especially the semicrystalline isomer (L-lactide, PLLA), is regularly used in medical device applications. PCL is well represented in many applications where longer degradation times would be allowed or desired.[11,12] PCL is established as a low-melting-point material that is readily soluble in many solvents used in ES.[1,13−15]

PLLA has also been utilized historically by blending it with modifiers or copolymerizing it with other resorbable monomers to create a more elastic polymer.[16−18] Standard ratios for PLLA and PCL copolymers are in the ranges of 30% ε-caprolactone and 70% L-lactide.[19−22] These copolymers have provided intermediate property materials for medical device development, where applications required optimized softness and strength. PLA, PCL, and their copolymers are resorbable polymers adaptable to processing via several modes of AM including, but not limited to, material extrusion (MEX), electrospinning (ES), and to a lesser extent powder bed fusion (PBF).[23−26] MEX includes processes previously referred to as fused filament fabrication (FFF), fused deposition modeling (FDM), and other thermal/chemical means of providing material through an orifice. PBF encompasses selective laser sintering (SLS). This compatibility with absorbable polymers uniquely positions AM processing modes for the design of temporary scaffolds.[27]

A new paradigm in medical, material, and tissue engineering research has followed an idea that appropriate mimicry of the target tissue would not only result in reduced time required for healing but also offer a regenerative approach that results in less contracture and scarring.[28,29] As the scaffold degrades or is resorbed, the new tissue would provide the functionality of the original tissue by regenerating the morphology of healthy tissue.[20,28,29] AM methodologies, such as ES, are proven to be well-suited to using aliphatic polyesters to make absorbable scaffolds with optimizable porosity and, due to the range of resorbable polymers available, the mechanical properties and degradation rates are widely varied.[30−34]

Electrospinning (ES) was established as a fiber formation process that could be used with a wide range of medical-grade materials.[5] Despite the desire to produce tissue-like scaffolds with the large range of material options, ES is challenged as a viable manufacturing method.[35−37] Lack of stability and clinical risks of surgical complications related to unproven technologies have caused a hesitation to transition the standard of care to ES products. Engineering an ES product requires monitoring and control of a seemingly countless amount of input parameters and critical quality control characteristics. ES parameters are not limited to the voltage, distance to collector, and dispensing rate but also include the solution properties, equipment properties, and even environmental properties, such as air flow rate and humidity. All of the parameters are critical to optimizing production processes and also have strong interactions with each other that must be accounted for to produce a controlled product. Solution properties are impacted by the polymer molecular weight, polydispersity, and concentration. The electrical properties of the polymer and solvent(s) also play a critical role in the process requirements. The combination, and harmony, of this overwhelming list of effective process parameters has been used to create successful devices that mimic natural structures and improve patient outcomes.[38−40]

While the material properties of a resorbable material would be selected during the early design phase of device development, these materials are historically plagued by sensitivity to process impacts on their properties.[3,41−44] Thus, combining an ES layer upon layer manufacturing with resorbable materials such as aliphatic polyesters has proven to be a tortuous path but also a novel opportunity to optimize and modulate properties with a wide range of critical input parameters available. However, the resulting properties of the final implant can be significantly different from what the clinician intended. Therefore, material selection must be done with processing parameters in mind. Many bioresorbable materials have been electrospun into scaffold structures and are established in clinical medical devices.[45,46] Electrospinning PLLA, PCL, and copolymers of these has been shown to be a safe and effective method of producing improved devices.[11,47] Despite this success, additional understanding is still required for continued translation of optimized devices to the clinic.

In this work, electrospinning of medical -grade polymers, PLLA, PCL, and a copolymer (Lactoflex), from hexafluoroisopropyl alcohol (HFIP) was performed using a targeted range of process parameter combinations to create modulated structures that exhibited a range of mechanical properties. Preliminary work is documented in the Supporting Information, including how to define parameter boundaries for electrospinning equipment and extensive statistical analysis. The screening investigated the parameter effects and interactions with the scaffold structures and properties. The orthogonal experiments and nonlinear regression of the multivariable data set resulted in a set of process parameters applicable for all three materials to modify the scaffold structures and create three overlapping mechanical property ranges. The parameter interaction of the solution dispensing rate with the dispensing distance to a rotating collector resulted in a large range of random nonwoven densities. Relatively high dispensing rates were combined with low collection distances into a parameter setting that resulted in "high" density samples. Relatively low dispensing rates and longer collection distances resulted in lower density samples. The conclusions were general trends of how the parameters impact the resulting fiber arrangement. Different equipment could require alternate settings to recreate the results, but the trend was concluded to be valid. The samples and structures were physically and mechanically characterized to allow a comparison of both the materials and the ES parameter effects. Within material groups, density was observed to correlate with mechanical properties, and the parameter control allowed property control. Softer (ε-caprolactone) and stiffer (L-lactide) homopolymer materials, previously known to the field of AM and ES, were compared. The impacts of the process parameter manipulation were also shown with an intermediate copolymer material, Lactoflex. The goal of this work was to use a subset of medical-grade materials and control a minimized number of critical process parameters to produce a maximized, optimizable, and predictable mechanical property range.

MATERIALS AND METHODS

Medical-Grade Polymers and High-Purity Solvent. Caproprene 100M (PCL), Lactoflex 7415, and Lactoprene 100M (PLLA) were synthesized by ring opening polymerization, ground into a polymer chip, and provided by PolyMed, Inc. Caproprene is a homopolymer of ε-caprolactone, and lactoprene is a homopolymer of L-lactide. Lactoflex is a

https://doi.org/10.1021/acsomega.4c01864
ACS Omega 2024, 9, 36982−36992

copolymer of ε-caprolactone, L-lactide, and trimethylene carbonate (TMC). Each medical-grade material was characterized to verify conversion to the polymer by residual quantification, inherent viscosity, and thermal melting analysis. Hexafluoroisopropanol (HFIP) solvent was sourced from Apollo Scientific.

Preparation of Polymer Solutions. Polymer granules were dissolved with HFIP in glass bottles on rollers for 40−80 h. Dissolution occurred within a fume hood. Nominal concentrations were determined by viscosity-targeting interpolations. Solution viscosity determinations were made using a RheoSense MicroVisc instrument at 25 °C and 100 s^{-1}. The resulting solutions (400−600 Pa·s) were transferred from the glass bottles to sterile syringes and subsequently used for electrospinning.

The Electrospinning Enclosure. A custom enclosure was utilized to execute the ES runs. The enclosure housed a traversing needle bed, a rotating collector (drum), and programmable syringe pumps. Four needles in parallel were used to generate the samples in this work. The enclosure utilized a multineedle array that allowed up to 8 needles in use at a time. The aluminum-based array utilized set-screws to secure the 20-gauge blunt-end needles and ensure repeatable electrical connections to each. The needle array was electrically connected to a direct current high voltage source (Matsusada Precision), and the rotating collector drum was electrically connected to the ground of the system. Prior to ES, the needle to drum distance (NTDD) was user-determined and maintained visually. The enclosure was operated at 15−35 kV within an ISO class VII cleanroom maintained at 6 Pa positive pressure, 50−65% RH, and 21 °C.

Electrospinning Parameters. Solution viscosity, needle and collector rates of motion, and voltage settings were optimized via Plackett−Burman screening and full factorial analysis of the parameter effects. Settings were required for each material to generate successful samples at three (3) separate densities. Optimization included mechanical testing, dimensional analysis, visual inspection of fibers and scaffold, and basis weight targeting. By targeting the mass of material collected relative to the collection area, it was ensured that the scaffold samples would be sufficiently sized for removal from the collector and could be loaded repeatably into the tensile analysis fixture. It was understood that the specific settings used would relate to the custom equipment and enclosure used for electrospinning. The scientific and engineering goal was to establish which parameter(s) and direction(s) had effect(s) that could be modulated to control properties and performance.

Non-Woven Scaffold Basis Weight (AD, Areal Density). The electrospun scaffold was cut into 51 mm × 102 mm samples in both the machine and countermachine directions. An engineering scale with 0.1 mm resolution was used to verify the dimensions prior to observing the mass at 0.1 mg with a Mettler Toledo (Columbus, OH) digital balance. An Ames comparator with a 25 mm pressure foot and no added mass was used to measure the thickness of the scaffolds. NIST traceable calibrations and standards ensured the accuracy of the measurements.

Thermal Analysis. Differential scanning calorimetry was performed with a PerkinElmer 6000 autosampler (Waltham, MA). Two stage cooling allowed observations of the lower PCL transitions. Heat rates were set to ramp up 10 °C/min until the thermal events for 5−6 mg samples concluded to allow visually selected heat of fusion (J/g) and peak melting temperature (°C) determinations within the Pyris software.

Molecular Weight Analysis. Size exclusion chromatography (SEC) was used to determine molecular weights (MWs) and polydispersity (PD) relative to polystyrene calibration standards with a Waters Breeze system (Milford, MA). The system was equipped with a refractive index detector (model 515) and several gel permeation chromatography (GPC) columns (Sytragel HR 0.5, 2, 4, and 6) in series. Using a 1 mL/min flow rate of the methylene chloride (DCM) mobile phase, samples with a concentration of 4 mg/mL (n = 3) were analyzed using user-defined integration of the resulting chromatograms within the Breeze software.

Confirmation of Material Compatibility via Cytotoxicity. Each material was tested as an electrospun scaffold (n = 3) by a third-party service according to ISO 10993-5 Biological Evaluation of Medical Devices Part 5; tests were done for *in vitro* cytotoxicity. Using a ratio of 0.2 g/mL, extractions were performed at 37 °C for 24 h so each seeded cell culture plate could be used with unmodified extract fluid. After 48 ± 3 h of incubation at 37 ± 1 °C, intracytoplasmic granules and cell lysis were quantified and combined into a single 0−4 score, with 0 representing the lowest toxicity result relative to a positive and negative control.[41]

Tensile Mechanics. Mechanical properties were quantified by tensile extension to failure with an MTS Criterion Model 43 test frame (Eden Prairie, MN). A 500 N load cell ensured that the 0.4 N/1% accuracy was sufficient for the study's observations. Advantage Pneumatic Action grips (Eden Prairie, MN) and smooth rubber face plates (as described in ASTM D5034) were used to clamp each sample with a pressure of 0.2 MPa and then strain at 100 mm/min from a gauge length of 38.1 mm (see Figure 1).[48] Five (5) tests to failure were performed for each test group, and the TestWorks software provided stress and modulus calculations based on the previously described dimensional observations.

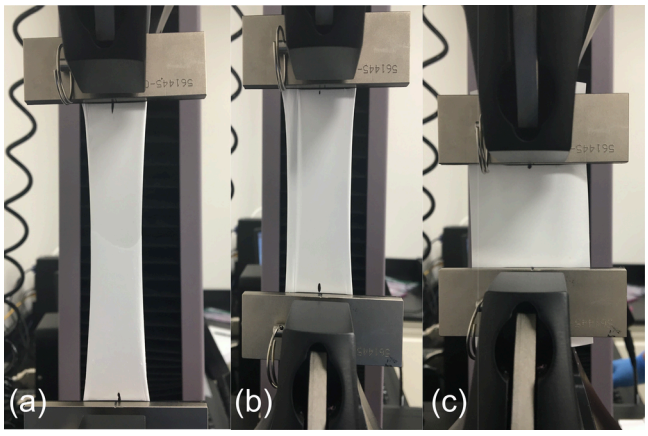

Figure 1. Medium density electrospun during tensile testing at maximum strain: (a) caproprene, (b) Lactoflex, and (c) lactoprene

Gas Chromatography. Two types of gas chromatography were used for this study. They both utilized PerkinElmer Clarus 580 GC instruments with DB 624 columns and heat ramp methods to facilitate the separation of the component analytes. For residual monomer analysis, the polymer was dissolved in HFIP prior to the manual injection into the GC inlet. The observed chromatograph was compared to external calibration curves generated with prepared monomer standards

https://doi.org/10.1021/acsomega.4c01864
ACS Omega 2024, 9, 36982−36992

in HFIP. This method was found capable of achieving quantification limits for each monomer relating to less than 0.1% weight/weight monomer in polymer. Residual HFIP was determined by multiple headspace extraction using a PerkinElmer TurboMatrix GC inlet attachment. Four extractions were sufficient to determine a total solvent content calculation as compared to external calibration with prepared HFIP standards in water. This method was found capable of achieving an HFIP quantification limit relating to less than 100 ppm solvent in polymer.[49]

Scanning Electron Microscopy (SEM). Micrograph images were obtained using a Hitachi 3400 SEM calibrated to a 10 mm working distance. Platinum-coated samples were imaged at 2000× and 200× using 15 kV with 125 μA emission current and 40 μA probe current set to the 10 mm working distance. Note: due to the thin nature of the samples, the actual working distance could be up to 11 mm to maintain image focus. To remove user error and bias, software was trained and programmed to identify the fibers in the focal plane of an SEM image and to measure the fiber diameter relative to the scale provided in the image by the SEM software. Automated analysis of the images was performed using Clemex Vision PE software with a custom-programmed Clemex.ai program for segmentation of the fiber micrographs.

Statistical Analysis. MiniTab version 18.1 (State College, PA) was used to perform one-way analysis of variance (ANOVA) on all data sets collected with α = 0.05 to determine significant differences with either Tukey or Games−Howell methods (based on equal variance F-test results). The two-sample t test was used to generate P-values. The design of experiment (DOE) methods were also used to perform orthogonal screening of process variables (see the Supporting Information). The error bars depicted indicate a single standard deviation above and below an average of five replicates. Additional statistical analysis was performed with MiniTab to design, model and predict critical parameters when preparing the study.

RESULTS

Electrospinning parameters were screened for critical impact on density and subsequent mechanical properties of the resulting nonwoven scaffold using caproprene, lactoflex, and Lactoprene materials (see Supporting Information Figures S15−S19). The solution dispensing rate parameter had an inverse effect and an interaction with the collection distance parameter, and combined they allowed a maximized effect range for density and corresponding mechanical properties. The use of a "high" dispensing rate with a shorter distance to the collector was deemed the high-density setting. Thus, the "low" dispensing rate and further collection distance were the low-density setting, with median values of each being referred to as the medium density setting. The matrix of three materials and three density settings (Figure 2a) resulted in nine (9) unique parameter combinations for scaffold production by electrospinning (ES). Each sample was characterized to allow observations of the material and parameter effects on the scaffold structure and mechanical properties.

Solution Preparation, Parameter Selection, and Fiber Formation. The prepared polymer solutions in HFIP were analyzed to determine concentration versus viscosity curves (see Supporting Information Figure S1. The solutions from each viscosity data point were then dispensed from a syringe through the charged ES needle to visually scope the

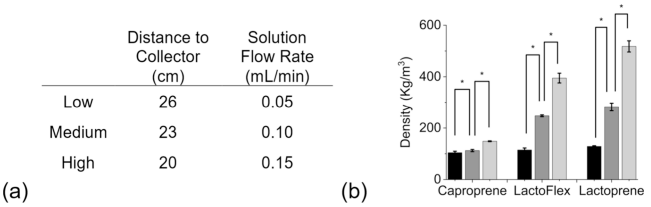

Figure 2. Defining the ES Scaffolds. (a.) The parameter selections. (b.) The low- (black), medium- (gray) and high-density (light gray) samples. (N = 5, error bars represent a single standard deviation). Statistically significant groups are indicated above the data (α = 0.05, *P < 0.01).

spinnability for each solution type and viscosity. This prescreening was performed by inspecting microscope slides held in front of the collector. The usable ranges of each process parameter relative to the other parameters, such as distance to collector, voltage, and solution flow rate, were observed with visual confirmation of the fiber-covered slides. This resulted in the maximums and minimums provided for the statistical screening (see Supporting Information Tables S1 and S2). The feasible fiber formation ranges were needed to screen process parameters utilized for scaffold sheet formation such as traversing rate, collector spinning rate, number of needles in the charged array, and total mass of polymer dispensed (see Supporting Information Figures S2−S13). Screening parameters within the observed feasible ranges resulted in the most critical and modular parameters with respect to the tensile mechanics to be selected for this study (see Supporting Information Figures S14−S19).

Electrospinning Scaffold Parts. The process parameters were screened via the Plackett−Burman design of experiment methodology to determine the most impactful parameter(s) for mechanical property control with the minimum possible number of scaffold sheets. Analysis of tensile mechanics and dimensional parameters of the initial screening sheets of the scaffold led to a need for slightly more information about the main effects observed for the process, the needle-to-drum distance (NTDD), and pump flow rate parameters. Adding center point runs for these parameters created a pseudofull factorial study matrix for what was found to be the critical parameters that affected the tensile mechanics, especially the modulus of the scaffold sheets, by controlling the scaffold density and porous structure. Spinning parameters were selected to optimize for the ranged inputs to result in structural variation observed and quantified as the scaffold densities (see Figure 2). Based on the initial screening results, the study focused on two critical parameters for controlling the effective density of the electrospun scaffolds: (1) the solution dispensed flow rate per needle and (2) the proximity of the grounded collector to the high voltage charged needles (NTDD).

All three of the groups in Figure 2b had statistically significant low, medium, and high densities observed that overlapped with the other material ranges. The use of a longer distance for the fibers to self-repel with a slower dispensing rate in Figure 2a produced a loftier, more porous scaffold versus the higher fiber packing density when dispensing higher flow rates more proximal to the collector. The trend held when an intermediate setting for each parameter was used.

Visual inspection included the unaided eye as well as SEM imaging at both 200× and 2000× magnification. Dimensional properties of thickness (±0.002 mm) and mass (±0.0001 g)

https://doi.org/10.1021/acsomega.4c01864
ACS Omega 2024, 9, 36982−36992

Table 1. Thermal and Molecular Analysis Results ($N = 3 \pm SD$)

		glass transition (±1 °C)	melting temperature (±1 °C)	enthalpy of melting (±2 J/g)	number-average MW (kg/mol)	PD	residual monomer content (wt %)
caproprene 100M	polymer chip	−62.5	57.9	69.7	97 ± 0.6	1.5	0.11 ± 0.01
	electrospun scaffold	−62.0	57.1	55.0	102 ± 1.3	1.5	0.01 ± 0.00
Lactoflex 7415	polymer chip	23.5	172.7	50.0	172 ± 4.3	1.8	0.51 ± 0.03
	electrospun scaffold	33.4	159.5	20.5	193 ± 12.9	2.0	0.04 ± 0.00
lactoprene 100M	polymer chip	74.4	188.3	83.2	132 ± 0.6	1.4	0.06 ± 0.00
	electrospun scaffold	71.2	177.2	41.3	131 ± 5.0	1.4	0.02 ± 0.01

confirmed low-, medium-, and high-density scaffolds were produced for each material. The density measurements in Figure 2b confirmed the target low-, medium-, and high-density scaffolds were produced as hypothesized per the screening matrix results.

To ensure that the scaffolds best represented the density control for each material, the solvent content was measured by multiple headspace extraction gas chromatography. The use of this methodology prevented the need for matrix matching across the multiple materials and constructs.[49] It was observed that caproprene scaffolds did not contain any detectable residual solvent after standard reduced pressure storage, which protects the material from ambient moisture-driven degradation. Lactoflex and lactoprene, however, were observed to retain as much as 10% HFIP by weight until being dried by reduced pressure overnight at a temperature of 70 °C. This temperature aligned with the onset of glass transition by DSC (Table 1). The drying was sufficient to ensure that both materials no longer contained detectable residual solvent.

Thermal analysis of the materials aided in the selection of the drying temperature. Additional thermal analysis was performed to begin the investigation of the processing effects on the materials. Table 1 contains the materials' glass transitions and melt temperatures as polymer chip and as dried electrospun scaffolds, in addition to molecular weight (MW) and polydispersity (PD) data.

Table 1 also includes the relative molecular weight by SEC and residual monomer by GC observations. Thermal property measurements were aligned with expectations for these materials. Processing results in lower melting temperatures, and the fiber enthalpy of melting is consistently observed to be lower than that of the polymer chip with or without heated drying. This is likely related to the ring-opening synthesis used to produce the polymer chip materials. While the molecular weight change did not suggest gross degradation of the material, an interesting effect of ES was noted. There was a decrease in the residual monomer detected and a correlated increase in glass transition temperatures. Removal of low-molecular-weight components was also observed to potentially result in a higher reported molecular weight polymer. However, the monomer content of the chip was not observed to impact fiber formation during the process. Residual content, such as monomer and solvent, and degradation were considered factors in the potential cytotoxicity of the scaffold samples. The results of the cytotoxicity analysis were used to generate Table 2.

All three materials were scored the same as the negative control, confirming the materials were not cytotoxic. This provided the confidence in the scaffold samples to continue with the physical characterization.

Table 2. Electrospun Scaffold Cytotoxicity Results

material	sample	negative control	positive control
caproprene 100M	0	0	4
Lactoflex 7415	0	0	4
lactoprene 100M	0	0	4

Dimensions of Electrospun Scaffold Samples. Scanning electron microscopy (SEM) micrographs were analyzed via Clemex Vision PE and Clemex.ai software to determine the fiber diameters and pore sizes. Clemex.ai was able to segment the top fiber layer, fiber edges, and pores in the SEM micrographs and allowed Vision PE to automate the measurement process. The average diameters of the fibers in each image were formed into histograms and tabulated (Table 3 and Table 4). A table of fiber analysis figures was produced instead of presenting a large number of figures, and this method was found more conducive to making the desired comparisons.

The fiber diameter distributions in Table 3 included 3000−8000 diameter measurements per sample, allowing observations of the impact of the low, medium, and high combinations of critical parameter settings (distance to collector and flow rate) on the fiber diameter. The three fiber size populations were observed to be statistically different with 95% confidence for each material using a one-way ANOVA Tukey test. A general trend of increasing fiber size was observed down each column in Table 3 and was associated with the increase in density. Literature reports showed that the increased fiber diameter was a result of either reducing the distance to the grounded collector or dispensing the solution faster.[50] The trend was only observed in Lactoflex and lactoprene. The caproprene scaffold images indicated the opposite trend, but a review of the fiber size data (left column of Table 3) revealed a bimodal distribution that could account for trend deviations. The 2000× micrograph was assessed to confirm this finding. The goal of this study was to relate the structure of the scaffold, as quantified by the density, to the potential for mechanical property control and not to produce monodisperse fiber structures. Representative micrographs of the samples used for the analysis were found and arranged for all nine (9) samples in Table 4.

The ultrathin fibers that would result in the bimodal distribution were obvious in the 2000× micrographs of the left column of Table 4. All nine (9) micrographs visually confirmed the range of scaffold structures that were produced.

Tensile Mechanics. The mechanical properties of each scaffold group were quantified by constant-strain rate tensile analysis to observe the comparative effect of varying-process-parameter-determined structural modulation. By measuring the

https://doi.org/10.1021/acsomega.4c01864
ACS Omega 2024, 9, 36982−36992

Table 3. Fiber Diameter Distributions for Electrospun Scaffolds

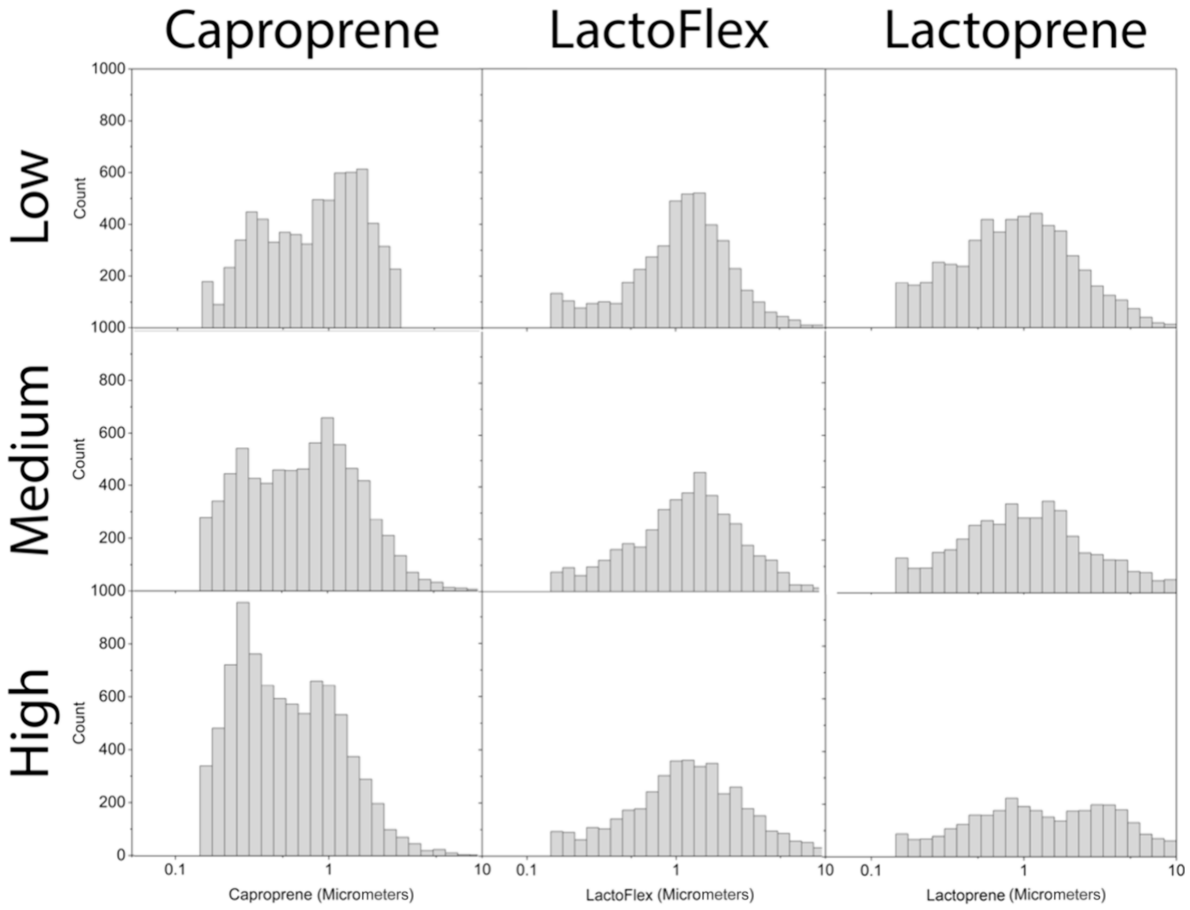

load required to strain the scaffold samples to failure, the ultimate tensile strength (UTS) and Young's tensile modulus were determined relative to the overall dimensions of the test sample within the Testworks software (see Figure 3a and b, respectively).[48]

Figure 3 a and b allowed the effect of density and scaffold structure on the mechanical strength and stiffness to be observed. The data in Figure 3 were combined to form an Ashby plot (Figure 4), exposing the process−structure−property relationship between ES process parameters, the structural density of the produced scaffold, and the resulting mechanical properties.

An approximately linear trend was observed as expected based on a previous AM parameter investigation.[41] The images in Figure 1 are representative of the deformation for each material group prior to the subsequent failure and UTS observation. Caproprene scaffolds were weaker, softer, and more elastic than the other two materials, as expected based on bulk material properties well-known to the homopolymer PCL. Similarly, the lactoprene scaffolds were stronger, stiffer, and more brittle than the other two materials, as expected for PLLA. However, both homopolymers were significantly weaker and softer than properties known for the bulk materials. The mechanical properties for low-, medium-, and high-density samples were found to be statistically different by one-way ANOVA Tukey test with 95% confidence for each material. The range of mechanical properties for Lactoflex at low, medium, and high density was observed to span from the PCL range to the PLLA range, as expected for the intermediate copolymer material. Each material was observed to follow the trend of increasing properties with increased density due to the ES process parameter control. The rate of densification and modulation of properties were not equivalent for each material. Stiffer materials proved more sensitive to the parameter range utilized for this study.

DISCUSSION

This study investigated the use of electrospinning (ES) porous scaffold structures with medical-grade aliphatic polyesters. Bioresorbable polymers, including those in this study, provide a unique option to clinicians where long-term risks and follow-up explantation can be significantly reduced to as low as zero.[51] These materials were used with electrospinning (ES) to make bioresorbable scaffold structures. The control of critical process parameters resulted in control of the scaffold structural density and, subsequently, control of the scaffold stiffness. The ability to target any stiffness in a biologically relevant property range was shown with only a few materials. This would suggest that more appropriate and targeted scaffolding could be manufactured to mimic biological tissue and potentially improve outcomes for patients in terms of tissue function and healing time through a deeper investigation into currently available medical-grade materials.

Many assume and have concluded that additive manufacturing (AM), especially ES, is a not a viable mode of manufacturing.[30,50,52] If the mechanical properties of bioresorbable polymers, especially aliphatic polyesters, were better understood, optimized, and considered in relation to

https://doi.org/10.1021/acsomega.4c01864
ACS Omega 2024, 9, 36982−36992

Table 4. Micrographs for Electrospun Samples

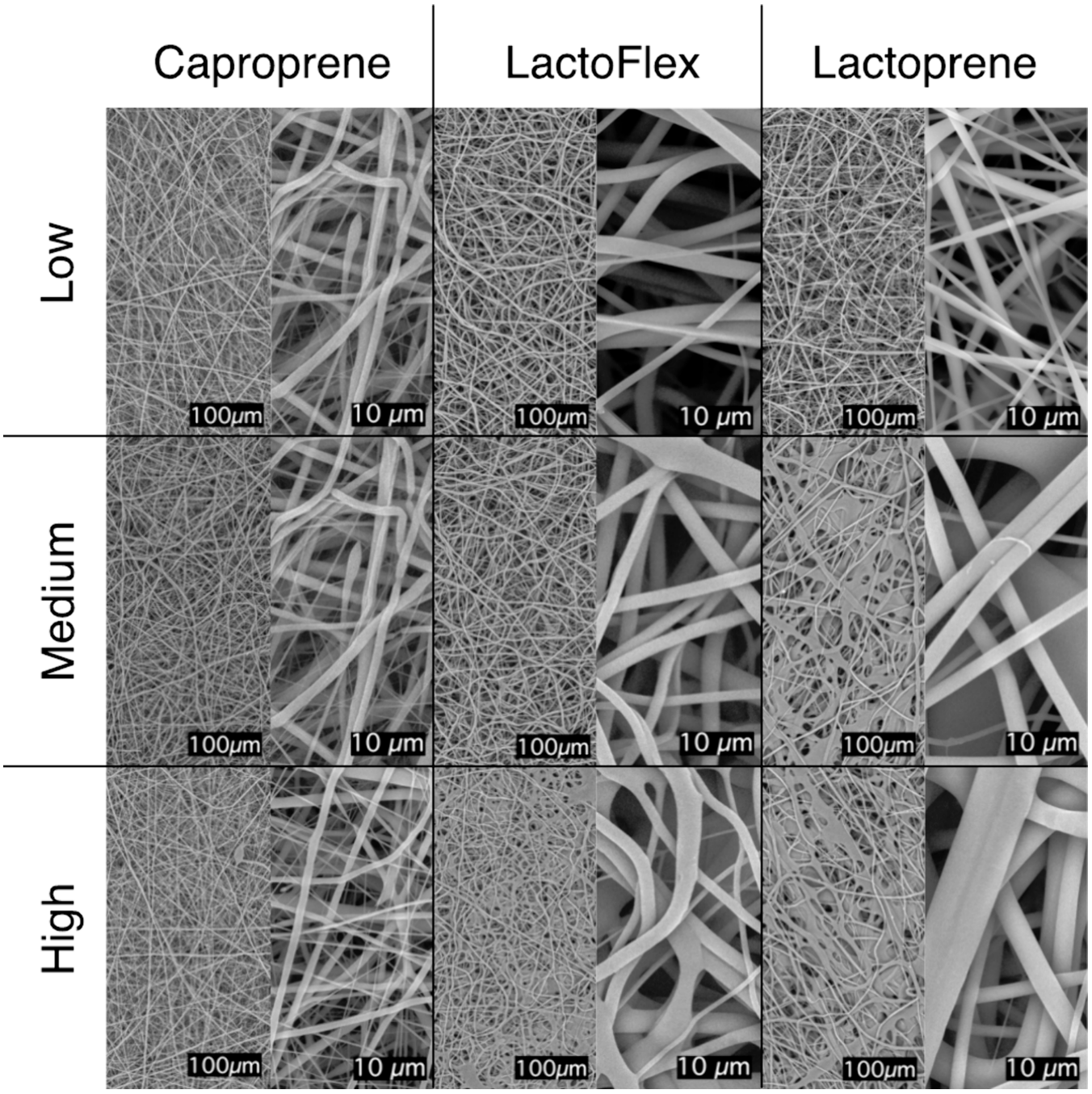

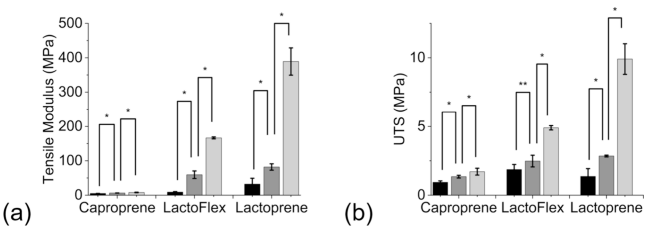

Figure 3. Electrospun scaffold mechanics versus low- (black), medium- (gray), and high-density (light gray) samples. (a) Young's tensile modulus and (b) ultimate tensile strength (UTS) ($N = 5$, error bars are one standard deviation). Statistically significant groups are indicated above the data ($\alpha = 0.05$, $^{*}P < 0.01$, $^{**}P < 0.02$).

processing parameters, those assumptions could be challenged. The stiffness of bulk poly L-lactide (PLLA) in terms of the tensile modulus (2.8−3.6 GPa) has been associated with the biological material properties of both the trabecular bone and the low end of cortical bone (0.76−10 GPa and 3.3−20 GPa, respectively).[53] This has also been confirmed clinically in maxillofacial applications such as bone screws and scaffolds, especially with ceramic-based additives such as tricalcium phosphate (TCP).[54,55] While the stiffest sample produced for this study, PLLA "high" density, was 389 MPa and would not be ideal for bone without further modification, electrospinning of the medical materials based on PLA and PCL was shown to produce materials exhibiting tensile modulus values relating well to soft tissue such as skin (0.3−140 MPa) and collagen

https://doi.org/10.1021/acsomega.4c01864
ACS Omega 2024, 9, 36982−36992

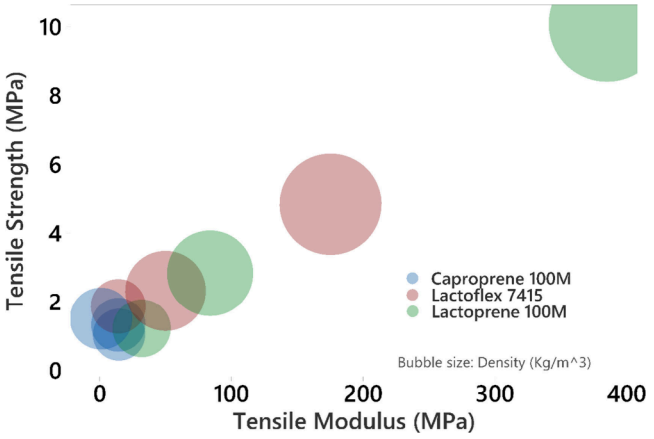

Figure 4. Ashby plot of tensile modulus vs tensile strength indicating the range of tensile mechanics observed for caproprene (blue), Lactoflex (red), and lactoprene (green) electrospun samples.

(70−110 MPa).[56−59] Due to the relatively large property range for skin, the parameter-controlled potential observed in this study should be critical to the optimization of scaffolds for soft tissue. The sensitivity of the structure and properties of AM and ES scaffolds to process parameters further bolsters the regulatory requirements for the full characterization of medical devices and AM devices. This includes but is not limited to the residual content quantifications, thermal and molecular properties, and material identity confirmations.[60,61]

The potential for process parameter optimization of output mechanical properties could result in the understanding required to further implement bioresorbable materials such as aliphatic polyesters into standard-of-care medical devices that exceed current expectations for wound care and other tissue engineering and regenerative medicine (TERM) applications. This potential has been both reported and refuted in more current literature, suggesting the nuance and difficulty involved in the ideal execution of TERM requirements. Many have reported ES-produced scaffolds as interesting due to the structural similarities to the extracellular matrix but ultimately without proven usefulness. The proposed solution has been that new material options would advance the use of ES as a production method. However, extensive investigation into process parameters and their interactions as control opportunities, not limitations, could offer the desired advancement. The skeptical conclusions likely compared AM production methods at the current level of understanding to the nearly ancient methods of molding and subtractive manufacturing. Milling and molding have proven themselves capable of mass production of optimized products. This was not achieved without a great deal of investigation and understanding gained over the long life span of these techniques. While those processes do have parameters that impact structure and resulting properties, they do not allow the novel designs, especially internal porosity control, that position AM to produce designs that were previously not possible without layer upon layer construction.

Using ES parameters and interactions such as the proximal distance to the collector combined with the solution dispensing speed, an extensive range of properties was observed, which was much less limited by the number of materials provided than previously understood. Full characterization of the thermal and molecular properties of the materials throughout the processing steps allowed for the observation that degradation was not a concern for the ES mode of production with aliphatic polyesters. The cytotoxicity risk of all three materials used to produce scaffold samples was minimized by including this analysis in the characterization of the study samples. This new understanding of ES and these materials has revealed a potential for new frontiers, with currently available materials providing the necessary properties for successful TERM device development.

Future work with PCL, PLLA, and copolymers of the like should continue to investigate process impacts on the mechanical properties of AM scaffolds so that a fuller understanding can be applied to device design and optimization toward target properties. Post-processing steps such as heat treatment and sterilization have been shown to have dramatic effects on initial properties as well as strength retention through the degradation cycle. Sterilization techniques such as radiation treatments with γ-rays have been used to significantly decrease the time required for degradation, but treatments with electron beam radiation would be recommended for less effect on the scaffold while further understanding is accrued.[62,63] An alternative to the highly criticized ethylene oxide (EO) treatments should also be investigated and is recommended. EO has a well-established history of minimal effect on products but poses other risks that are no longer readily acceptable for newly developed products and devices.[64,65]

ES was used to implement the control of process parameters, resulting in scaffolds with a range of densities and corresponding range of strengths and stiffnesses. With this understanding, precise control and optimization of scaffold mechanics could be developed into new device designs using a range of currently available medical-grade materials.

CONCLUSIONS

It was concluded that a novel scaffold device with targeted and optimized mechanical properties was feasible when applying a new understanding of electrospinning (ES) process parameter interactions and effects with currently available medical-grade materials. This biomimicry potential for wound healing applications and soft tissue repair was previously imagined for ES with a new material that is not currently available. ES parameter control of scaffold density and the resulting impact on mechanics using poly ϵ-caprolactone (PCL), an intermediate property copolymer (Lactoflex 7415), and poly L-lactide (PLLA) were evaluated to establish a feasible range of biomimetic mechanical properties. An even larger range of mechanics and biomimicry may also be feasible by including other materials, copolymers, additives, and/or biochemicals into the ES solution prior to electrospinning the scaffold. These would need to be evaluated as early as possible in the development process due to the initial process parameter tuning required for ES fiber formation. The ability to control and produce a range of properties with a single material was proven with three materials to result in a fully encompassing range of opportunities for property targeting. This control of scaffold properties could be further investigated for other materials as well as with other process parameters, such as post-processing steps. Sterilization effects on scaffold properties could have significant consequences that must be taken into account when designing a carefully targeted device property.

Electrospinning (ES) has been introduced as another mode of additive manufacturing (AM) for the three materials that

https://doi.org/10.1021/acsomega.4c01864
ACS Omega 2024, 9, 36982−36992

further expands the mechanical property targeting opportunities available for producing tissue scaffold structures with lactoprene 100M, Lactoflex 7415, and caproprene 100M.

■ ASSOCIATED CONTENT

Supporting Information

The Supporting Information is available free of charge at https://pubs.acs.org/doi/10.1021/acsomega.4c01864.

Additional methods, results, and minimal discussion outlining the process of selecting the dispensing rate and distance to the collector as interacting parameters to modulate the scaffold densities (PDF)

■ AUTHOR INFORMATION

Corresponding Author

O. Thompson Mefford − *Department of Materials Science and Engineering, Clemson University, Clemson, South Carolina 29634, United States; Department of Bioengineering, Clemson University, Clemson, South Carolina 29634, United States;* orcid.org/0000-0002-9164-2521; Email: mefford@clemson.edu

Authors

Clayton J. Culbreath − *Poly-Med, Inc., Anderson, South Carolina 29625, United States; Department of Materials Science and Engineering, Clemson University, Clemson, South Carolina 29634, United States*

Seth D. McCullen − *Poly-Med, Inc., Anderson, South Carolina 29625, United States; Department of Materials Science and Engineering, Clemson University, Clemson, South Carolina 29634, United States*

Complete contact information is available at: https://pubs.acs.org/10.1021/acsomega.4c01864

Notes

The authors declare the following competing financial interest(s): C.J.C. and S.D.M. are employed by Poly-Med, Inc., a producer of bioresorbable materials.

■ ACKNOWLEDGMENTS

Materials, equipment, laboratory space, and analytical capabilities were graciously provided by Poly-Med, Inc. for this study and its preliminary investigations. The authors would like to thank Jacob Rabinovitch and Lab Services at Poly-Med, Inc. for analytical assistance.

■ REFERENCES

(1) Youssef, A.; Hollister, S.J.; Dalton, P.D. Additive manufacturing of polymer melts for implantable medical devices and scaffolds. *Biofabrication* **2017**, *9*, 012002.

(2) Han, S.-K. *Innovations and Advances in Wound Healing*, 3rd ed.; Springer, 2023.

(3) *Electrospinning: From Basic Research to Commercialization*; Kny, E., Ghosal, K., Thomas, S., Eds.; Soft Matter; The Royal Society of Chemistry, 2018. DOI: 10.1039/9781788012942.

(4) Gugulothu, D.; Barhoum, A.; Afzal, S.M.; Venkateshwarlu, B.; Uludag, H. Structural Multifunctional Nanofibers and Their Emerging Applications. In *Handbook of Nanofibers*; Barhoum, A., Bechelany, M., Makhlouf, A. S. H., Eds.; Springer, 2019; pp 693−732. .

(5) Morris, H.L.; Martins, J.A.; Lach, A. A.; Carr, A.J.; Mouthuy, P.-A. Translational path for electrospun and electrosprayed medical devices from bench to bedside. In *Biomedical Applications of Electrospinning and Electrospraying*; Kasoju, N., Ye, H., Eds.; Elsevier Ltd, 2021: pp 423−454.

(6) Vonbrunn, E.; Mueller, M.; Pichlsberger, M.; Sundl, M.; Helmer, A.; Wallner, S.A.; Rinner, B.; Tuca, A.-C.; Kamolz, L.-P.; Brislinger, D.; Glasmacher, B.; Lang-Olip, I. Electrospun PCL/PLA Scaffolds are More Suitable Carriers of Placental Mesenchymal Stromal Cells Than Collagen/Elastin Scaffolds and Prevent Wound Contraction in a Mouse Model of Wound Healing. *Front. Bioeng. Biotechnol.* **2020**, *8*, 604123.

(7) Hoque, M. E. Robust formulation for the design of tissue engineering scaffolds: A comprehensive study on structural anisotropy, viscoelasticity and degradation of 3D scaffolds fabricated with customized desktop robot based rapid prototyping (DRBRP) system. *Mater. Sci. Eng. C* **2017**, *72*, 433.

(8) Barrientos, I. J. H.; MacKenzie, G.R.; Wilson, C.G.; Lamprou, D.A.; Coats, P. Biological performance of electrospun polymer fibres. *Materials* **2019**, *12*, 363.

(9) Chakroff, J.; Kayuha, D.; Henderson, M.; Johnson, J. Development and Characterization of Novel Electrospun Meshes for Hernia Repair. *SOJ Mater. Sci. Eng.* **2015**, *3*, 1−9.

(10) Mondal, S. S.; Griffith, D.; Venkatraman, M. Polycaprolactone based biomaterials for tissue engineering and drug delivery - current scenar-annotated.pdf. *Int. J. Polym. Mater. Polym. Biomater.* **2016**, *65*, 255−265.

(11) King, W. E.; Bowlin, G. L. Near-Field Electrospinning and Melt Electrowriting of Biomedical Polymers-Progress and Limitations. *Polymers (Basel).* **2021**, *13*, 1097.

(12) Woodruff, M. A.; Hutmacher, D. W. The return of a forgotten polymer - Polycaprolactone in the 21st century. *Prog. Polym. Sci.* **2010**, *35*, 1217.

(13) Brown, T. D.; Dalton, P. D.; Hutmacher, D. W. Melt electrospinning today: An opportune time for an emerging polymer process. *Prog. Polym. Sci.* **2016**, *56*, 116−166.

(14) Brown, T. D. *Melt Electrospinning Writing*. Doctoral Thesis, Queensland University of Technology, Brisbane, Queensland, 2015.

(15) Hollister, S.J. Scaffold Design and Manufacturing. *Adv. Mater.* **2009**, *21*, 3330−3342.

(16) Farah, S.; Anderson, D.G.; Langer, R. Physical and mechanical properties of PLA, and their functions in widespread applications — A comprehensive review. *Adv. Drug Deliv. Res.* **2016**, *107*, 367−392.

(17) Kessler, M.; Groll, J.; Tessmar, J. Application of Linear and Branched Poly(Ethylene Glycol)-Poly(Lactide) Block Copolymers for the Preparation of Films and Solution Electrospun Meshes. *Macromol. Biosci.* **2016**, *16*, 441.

(18) Lasprilla, A. J. R.; Martinez, G. A. R.; Lunelli, B. H.; Jardini, A. L.; Filho, R. M. Poly-lactic acid synthesis for application in biomedical devices - A review. *Biotechnol. Adv.* **2012**, *30*, 321−328.

(19) Shalaby, S.W. High Strength Fibers of L-Lactide Copolymers e-Caprolactone and Trimethylene Carbonate and Absorbable Medical Constructs Thereof. US 7192437 B2, 2007.

(20) Shalaby, S.W.; Burg, K.J.L. *Absorbable and Biodegradable Polymers*; CRC Press, 2005.

(21) Guerin, W.; Helou, M.; Carpentier, J. F.; Slawinski, M.; Brusson, J. M.; Guillaume, S. M. Macromolecular engineering via ring-opening polymerization (1): L-lactide/trimethylene carbonate block copolymers as thermoplastic elastomers. *Polym. Chem.* **2013**, *4*, 1095−1106.

(22) Callister, W.D. *Fundamentals of Materials Science and Engineering: An Interactive E-Text*; John Wiley & Sons, Inc., 2001.

(23) Lee, J. Y.; An, J.; Chua, C. K. Fundamentals and applications of 3D printing for novel materials. *Appl. Mater. Today.* **2017**, *7*, 120−133.

(24) Bose, S.; Ke, D.; Sahasrabudhe, H.; Bandyopadhyay, A. Additive manufacturing of biomaterials. *Prog. Mater. Sci.* **2018**, *93*, 45.

(25) Zadpoor, A. A.; Malda, J. Additive Manufacturing of Biomaterials, Tissues, and Organs. *Ann. Biomed. Eng.* **2017**, *45*, 1−11.

(26) Puppi, D.; Chiellini, F. Biodegradable Polymers for Biomedical Additive Manufacturing. *Appl. Mater. Today.* **2020**, *20*, 100700.

(27) Alghoraibi, I.; Alomari, S. Different Methods for Nanofiber Design and Fabrication. In *Handbook of Nanofibers*; Barhoum, A., Bechelany, M., Makhlouf, A. S. H., Eds.; Springer, 2019; pp 79−124.
(28) MacEwan, M.R.; MacEwan, S.; Kovacs, T.R.; Batts, J. What Makes the Optimal Wound Healing Material? A Review of Current Science and Introduction of a Synthetic Nanofabricated Wound Care Scaffold. *Cureus.* **2017**, *9*, No. e1736, DOI: 10.7759/cureus.1736.
(29) Rodriguez, J. C.; Chen, A. H.; Carney, D. E. Treatment of superficial second-degree burns with a nanofiber tissue matrix: A case report. *Burn. Open.* **2022**, *6*, 173−176.
(30) Garkal, A.; Kulkarni, D.; Musale, S.; Mehta, T.; Giram, P. Electrospinning nanofiber technology: A multifaceted paradigm in biomedical applications. *New J. Chem.* **2021**, *45*, 21508−21533.
(31) Harrison, R. H.; St-Pierre, J.-P.; Stevens, M. M. Tissue Engineering and Regenerative Medicine: A Year in Review. *Tissue Eng. Part B Rev.* **2014**, *20*, 1−16.
(32) Harrison, R. H.; Steele, J. A. M.; Chapman, R.; Gormley, A. J.; Chow, L. W.; Mahat, M. M.; Podhorska, L.; Palgrave, R. G.; Payne, D. J.; Hettiaratchy, S. P.; Dunlop, I. E.; Stevens, M. M. Modular and Versatile Spatial Functionalization of Tissue Engineering Scaffolds through Fiber-Initiated Controlled Radical Polymerization. *Adv. Funct. Mater.* **2015**, *25*, 5748.
(33) Santoro, M.; Shah, S. R.; Walker, J. L.; Mikos, A. G. Poly(lactic acid) nanofibrous scaffolds for tissue engineering. *Adv. Drug Delivery Rev.* **2016**, *107*, 206.
(34) Hinderer, S.; Layland, S.L.; Schenke-Layland, K. ECM and ECM-like materials - Biomaterials for applications in regenerative medicine and cancer therapy. *Adv. Drug Delivery Rev.* **2016**, *97*, 260.
(35) Bao, M.; Lou, X.; Zhou, Q.; Dong, W.; Yuan, H.; Zhang, Y. Electrospun Biomimetic Fibrous Scaffold from Shape Memory Polymer of PDLLA-co-TMC for Bone Tissue Engineering. *ACS Appl. Mater. Interfaces* **2014**, *6*, 2611.
(36) Freed, L. E.; Engelmayr, G. C.; Borenstein, J. T.; Moutos, F. T.; Guilak, F. Advanced material strategies for tissue engineering scaffolds. *Adv. Mater.* **2009**, *21*, 3410−3418.
(37) Sensini, A.; Gualandi, C.; Focarete, M.L.; Belcari, J.; Zucchelli, A.; Boyle, L.; Reilly, G.C.; Kao, A.P.; Tozzi, G.; Cristofolini, L. Multiscale hierarchical bioresorbable scaffolds for the regeneration of tendons and ligaments. *Biofabrication.* **2019**, *11*, 035026.
(38) O'Brien, F. J.; Christenson, L.; Ph, D.; Mikos, A. G.; Gibbons, D. F.; Picciolo, G. L. E. E. Biomaterials & scaffolds for tissue engineering. *Mater. Today.* **2011**, *14*, 88.
(39) Sears, N.A.; Seshadri, D.R.; Dhavalikar, P.S.; Cosgriff-Hernandez, E. A Review of Three-Dimensional Printing in Tissue Engineering. *Tissue Eng. Part B Rev.* **2016**, *22*, 298.
(40) Nikolova, M. P.; Chavali, M. S. Recent advances in biomaterials for 3D scaffolds: A review. *Bioact. Mater.* **2019**, *4*, 271−292.
(41) Culbreath, C.J.; Gaerke, B.; Taylor, M.S.; McCullen, S.D.; Mefford, O.T. Effect of infill on resulting mechanical properties of additive manufactured bioresorbable polymers for medical devices. *Materialia* **2020**, *12*, 100732.
(42) Can-Herrera, L. A.; Oliva, A. I.; Dzul-Cervantes, M. A. A.; Pacheco-Salazar, O. F.; Cervantes-Uc, J. M. Morphological and Mechanical Properties of Electrospun Polycaprolactone Scaffolds: Effect of Applied Voltage. *Polymers* **2021**, *13* (4), 662.
(43) Utela, B.; Storti, D.; Anderson, R.; Ganter, M. A review of process development steps for new material systems in three dimensional printing (3DP). *J. Manuf. Process.* **2008**, *10*, 96−104.
(44) Williams, D. F. There is no such thing as a biocompatible material. *Biomaterials.* **2014**, *35*, 10009−10014.
(45) Herrero-Herrero, M.; Gómez-Tejedor, J. A.; Vallés-Lluch, A. Role of Electrospinning Parameters on Poly (Lactic-co-Glycolic Acid) and Poly(Caprolactone-co-Glycolic acid) Membranes. *Polymers (Basel).* **2021**, *13*, 695.
(46) Chausse, V.; Casanova-Batlle, E.; Canal, C.; Ginebra, M. P.; Ciurana, J.; Pegueroles, M. Solvent-cast direct-writing and electrospinning as a dual fabrication strategy for drug-eluting polymeric bioresorbable stents. *Addit. Manuf.* **2023**, *71*, 103568.
(47) Xie, X.; Chen, Y.; Wang, X.; Xu, X.; Shen, Y.; Khan, A. ur R.; Aldalbahi, A.; Fetz, A. E.; Bowlin, G. L.; El-Newehy, M.; Mo, X. Electrospinning nanofiber scaffolds for soft and hard tissue regeneration. *J. Mater. Sci. Technol.* **2020**, *59*, 243−261.
(48) ASTM International. *Standard Test Method for Breaking Strength and Elongation of Textile Fabrics (Grab Test)*; ASTM D5034-21; West Conshohocken, PA, **2021**. DOI: 10.1520/D5034-21.
(49) Culbreath, C.J. *Quantification of volatile residuals in polydioxanone by gas chromatography: Method development, validation and implementation.* Master's Thesis, Clemson University, Clemson, SC, 2016.
(50) Haider, A.; Haider, S.; Kang, I. K. A comprehensive review summarizing the effect of electrospinning parameters and potential applications of nanofibers in biomedical and biotechnology. *Arab. J. Chem.* **2018**, *11*, 1165−1188.
(51) *Polymers of Biological and Biomedical Significance*; Shalaby, S.W., Ikada, Y., Langer, R., Williams, J., Eds.; ACS Symposium Series, Vol. *540*; American Chemical Society: Washington, DC, 1994. DOI: 10.1021/bk-1994-0540.fw001.
(52) Liu, H.; Gough, C.R.; Deng, Q.; Gu, Z.; Wang, F.; Hu, X. Recent advances in electrospun sustainable composites for biomedical, environmental, energy, and packaging applications. *Int. J. Mol. Sci.* **2020**, *21*, 4019.
(53) Wurm, M. C.; Möst, T.; Bergauer, B.; Rietzel, D.; Neukam, F. W.; Cifuentes, S. C.; von Wilmowsky, C. In-vitro evaluation of Polylactic acid (PLA) manufactured by fused deposition modeling. *J. Biol. Eng.* **2017**, *11*, 29.
(54) Drummer, D.; Cifuentes-Cuéllar, S. C.; Rietzel, D. Suitability of PLA/TCP for fused deposition modeling. *Rapic Prototyp. J.* **2012**, *18*, 500.
(55) Zhang, H.; Mao, X.; Du, Z.; Jiang, W.; Han, X.; Zhao, D.; Han, D.; Li, Q. Three dimensional printed macroporous polylactic acid/hydroxyapatite composite scaffolds for promoting bone formation in a critical-size rat calvarial defect model. *Sci. Technol. Adv. Mater.* **2016**, *17*, 136−148.
(56) Klinge, U.; Klosterhalfen, B.; Conze, J.; Limberg, W.; Obolenski, B.; Öttinger, A.P.; Schumpelick, V. Modified Mesh for Hernia Repair that is adapted to the Physiology of the Abdominal Wall. *Eur. J. Surg.* **1998**, *164*, 951.
(57) Ng, K. W.; Khor, H. L.; Hutmacher, D. W. In vitro characterization of natural and synthetic dermal matrices cultured with human dermal fibroblasts. *Biomaterials* **2004**, *25*, 2807.
(58) Broderick, G.; McIntyre, J.; Noury, M.; Strom, H. M.; Psoinos, C.; Christakas, A.; Billiar, K.; Hurwitz, Z. M.; Lalikos, J. F.; Ignotz, R. A.; Dunn, R. M. Dermal collagen matrices for ventral hernia repair: Comparative analysis in a rat model. *Hernia.* **2012**, *16*, 333.
(59) Kalra, A.; Lowe, A. Mechanical Behaviour of Skin: A Review. *J. Mater. Sci. Eng.* **2016**, *5*, 1000254.
(60) FDA. Guidance Document for Testing Biodegradable Polymer Implant Devices; U.S. Department of Health and Human Services: Silver Spring, MD, 1996; HHS-0910-1996-F-3812.
(61) Zuniga, J.M.; Major, M.J.; Peck, J.L.; Srivastava, R.; Pierce, J.; Stergiou, N. Technical and Clinical Considerations for the Development of 3D Printed Upper- Limb Prostheses for Children. In *Proceedings of the 3d Printing Conference Innovation, Modelling, Application & Implementation*, October 5−6, Las Vegas, NV; Allied Academics: London, U.K., 2017.
(62) Savaris, M.; dos Santos, V.; Brandalise, R. N. Influence of different sterilization processes on the properties of commercial poly(lactic acid). *Mater. Sci. Eng. C* **2016**, *69*, 661−667.
(63) *Irradiation of Polymers: Fundamentals and Technological Applications*; Clough, R.L., Shalaby, S.W., Eds.; ACS Symposium Series, Vol. *620*; American Chemical Society: Washington, DC, 1996.
(64) Mendes, G. C. C.; Brandão, T. R. S.; Silva, C. L. M. Ethylene oxide sterilization of medical devices: A review. *Am. J. Infect. Control.* **2007**, *35*, 574−581.
(65) Lerouge, S., Non-traditional sterilization techniques for biomaterials and medical devices. In *Sterilisation of Biomaterials and*

https://doi.org/10.1021/acsomega.4c01864
ACS Omega 2024, 9, 36982−36992

Medical Devices; Lerouge, S., Simmons, A., Eds.; Woodhead Publishing: Sawston, UK, 2016: pp 97−116. DOI: 10.1533/9780857096265.97

https://doi.org/10.1021/acsomega.4c01864
ACS Omega 2024, 9, 36982−36992